http://dx.doi.org/10.18623/rvd.v23.6641

NONLINEAR BEHAVIOR OF NON-COHESIVE SUBGRADE MATERIALS

COMPORTAMENTO NÃO LINEAR DE MATERIAIS DE SUBLEITO NÃO COESIVOS

Article received on: 1/18/2026
Article accepted on: 4/18/2026

Alexandr Lyapin*
***Don State Technical University, Rostov-on-Don, Russia
Orcid: https://orcid.org/0009-0001-6880-1598
lyapin.rnd@yandex.ru

Olga Shilyaeva*
***Don State Technical University, Rostov-on-Don, Russia
Orcid: https://orcid.org/0009-0008-1370-621X
o.shilyaeva@mymail.academy

The authors declare that there is no conflict of interest

Abstract
In the design of highway structures, it is important to take into account the behavior of soil and unbound subgrade layers. The model of nonlinear behavior of bulk materials, in this case sand, was used to describe the behavior of multilayer pavements, specifically the additional base layer. In this study, different variants of the extended Drucker-Prager model were considered to describe the static and dynamic behavior of the elements of a multilayer nonrigid roadway structure.

Keywords: Drucker-Prager Model, Nonlinear Behavior, Non-Cohesive Materials, The Finite Element Method.

Resumo
Na conceção de estruturas rodoviárias, é importante ter em conta o comportamento do solo e das camadas de subleito não ligadas. O modelo de comportamento não linear de materiais a granel, neste caso a areia, foi utilizado para descrever o comportamento de pavimentos multicamadas, especificamente da camada de base adicional. Neste estudo, foram consideradas diferentes variantes do modelo alargado de Drucker-Prager para descrever o comportamento estático e dinâmico dos elementos de uma estrutura rodoviária não rígida multicamadas.

Palavras-chave: *Modelo de Drucker-Prager. Comportamento não linear. Materiais não coesivos. Método dos elementos finitos.*

1 INTRODUCTION

When modeling the stress-strain state of objects on sandy soils, pavements containing layers of loose materials, an important aspect is the nature of the behavior of the base. As a rule, it is characterized by nonlinearity, significant dependence on compaction, the presence of liquid filtration in pores and dependence on the rate of dynamic impact (Kumar *et al*., 2012; Altun *et al*., 2006; Zhiqu *et al*., 2008). Known models describing the behavior of such materials are Coulomb-Mohr model, Drucker-Prager model, extended Drucker-Prager model, CAP-model and others. It also leads to

the need to create and apply new nonlinear models of sand behavior in different conditions (Bardet, 1990; Liu *et al*., 2021; Yin *et al*., 2018; Liao *et al*., 2025). One of the effective methods to study these models to verify their adequacy and compliance with experimental data is the finite element method, which takes into account the experimental conditions in detail (Alam *et al*., 2014; Abdullah, 2023; Fattah *et al*., 2013).

The greatest application of geotechnical modeling is found in FEM software packages such as Plaxis, SIMULIA Abacus, COMSOL Multiphysics, Ansys and others. In this paper, the inelastic behavior of materials such as sand, rock, and earth are considered using Ansys Mechanical APDL. The authors' application of finite element modeling in a problem for a two-layer environment can be found, for example, in the article (Babushkina *et al*., 2024).

In this study, different variants of the extended Drucker-Prager model are considered to describe the static and dynamic behavior of the elements of a multi-layer nonrigid highway structure. Different ways of describing the yield function and flow potential are considered, which can be linear, stepwise or hyperbolic:

$Q = q + \alpha\sigma_m - \sigma_Y(\hat{\varepsilon}_{pl})$ – linear flow potential; (1)

$Q = q^b + \alpha\sigma_m - \sigma_Y^b(\hat{\varepsilon}_{pl})$ – the potential of a power flow; (2)

$Q = \sqrt{a^2 + q^2} + \alpha\sigma_m - \sigma_Y(\hat{\varepsilon}_{pl})$ – hyperbolic flow potential. (3)

At the same time, the flow function can be chosen in one of three forms F=Q=0, with the flow function and potential type coinciding for the associated flow, and not coinciding for the non-associated flow.

Here q is the deviator of the Cauchy stress tensor;

$\sigma_Y(\hat{\varepsilon}_{pl})$ – yield strength of the material;

α – material constant determining the pressure intensity;

α, b – parameters characterizing the shape of the yield surface each in its own case.

Note that at $b = 1$ the step potential of plastic flow will coincide with the linear potential, and at $a = 0$ – the hyperbolic potential also passes to the linear potential.

2 METHOD

It should be noted that studies of static and dynamic behavior of non-bonded layers of the base of a multilayer structure of a non-rigid type highway were carried out within the framework of research and development work on the creation of a road test complex of the Federal Autonomous Establishment "ROSDORNII" designed for accelerated testing of roadways using the wheel load simulator "CYCLOS" (Konorev *et al.*, 2023).

Consider a constant surface pressure loading in the range of 0 to 318 KPa of wet sand filling an iron box with dimensions: 400x800 mm in plan and 300 mm deep (Figure 1).

The loading was carried out by uniform pressure over the entire surface with a 400x800 mm hydro pad.

The response of the medium was recorded by two pressure sensors (ultimate pressure up to 2 MPa) located in the center of the structure on the surface and at a depth of 75 mm. The diameter of the sensors is 200 mm.

Figure 1

An iron box with sand

2.1 Experimental details

To simulate the loading process in the Ansys APDL program, a geometric model of the structure has been created. To simplify the calculations, the axisymmetric

deformation of the medium was considered. The area is a cylinder 300 mm high and 400 mm in diameter. The medium material is sand at a relative humidity of 0.9.

The physical parameters of the material are summarized in Table 1.

Table 1

Static impact modeling

Designation	*Parameter name*	*Value*	*Unit*
E	Modulus of elasticity	100	MPa
v	Poisson's ratio	0.35	-
C	Modulus of adhesion	0.005	MPa
φ	Internal friction angle	31	degree
ψ	Dilatancy angle	0,15,31	degree
ρ	Material density	1850	kg/m^3
$\sigma_Y(\hat{\varepsilon}_{pl})$	Flow strength of the material	0.01035	MPa
α	Pressure intensity constant	1.244	-

Figure 2

Shows the finite element mesh of the study area. *Finite element mesh*

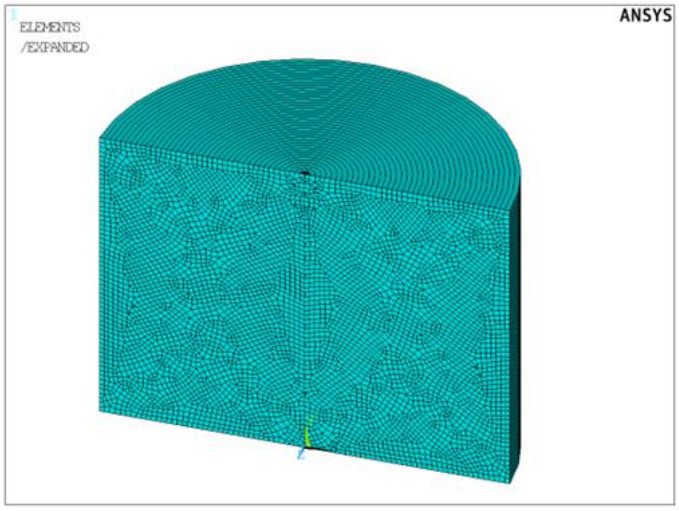

A study has been carried out to select the type and parameters of nonlinear material behavior in the extended Drucker-Prager model and their influence on the stress-strain state of the points of the considered model of a sandy foundation under loading by uniform surface pressure of intensity 318 kPa.

3 **RESULTS AND DISCUSSION**

Figure 3 shows the behavior of stress σ_Y as the observation point moves deeper into the structure from the surface at different values of the parameter b for the associated flow for the extended Drucker-Prager model for the power flow potential.

In Figures 3-6, the horizontal axis shows the depth of the observation point "H" in meters.

Figure 3

Compressive stresses σ_Y, Pa at parameter $b=1, 1.25, 1.5$

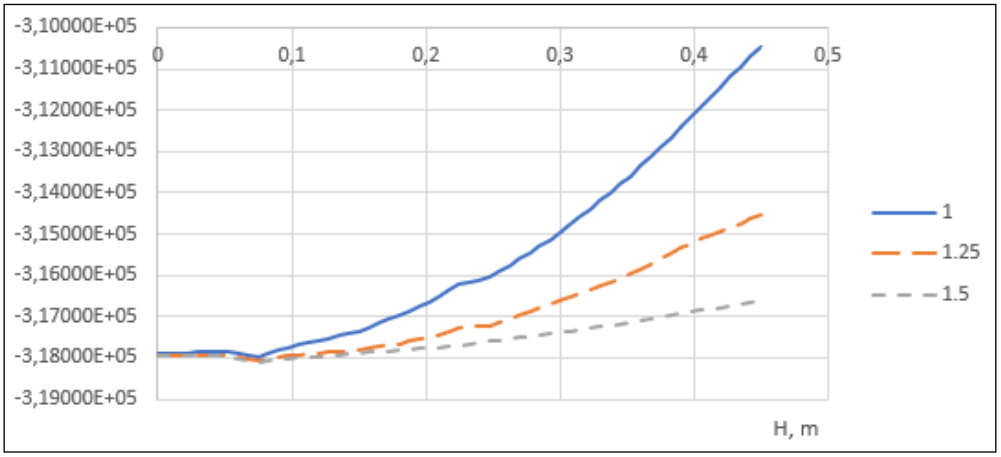

As can be seen from the figure, the power potential leads to a slower decrease in stress as it moves away from the upper surface of the structure with a given pressure. At the same time, significant changes can occur with the power parameter $b \in (1.1, 1.5)$.

Similarly, for vertical displacements, an increase in displacement values up to 100% is observed with the step law (Figure 4).

Figure 4

Vertical displacements Uy, m with distance into the structure at parameter b=1, 1.25, 1.5

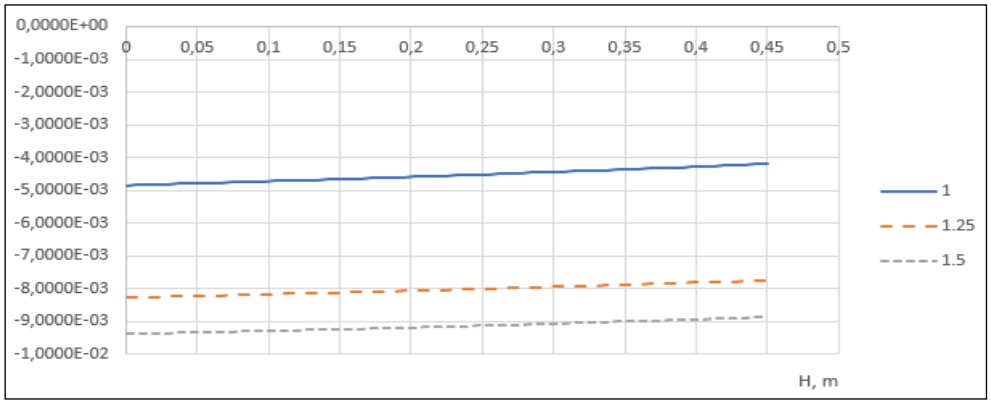

For hyperbolic yield function and hyperbolic flow potential, similar plots are presented in Figures 5 and 6 as a function of parameter $a = 0, 0.2C, 0.4C$. It is noted that in this case for the selected range of variation of this parameter the changes in the stress-strain state are insignificant.

Figure 5

Compressive stresses σ_y, Pa at parameter $a = 0, 0.2C, 0.4C$

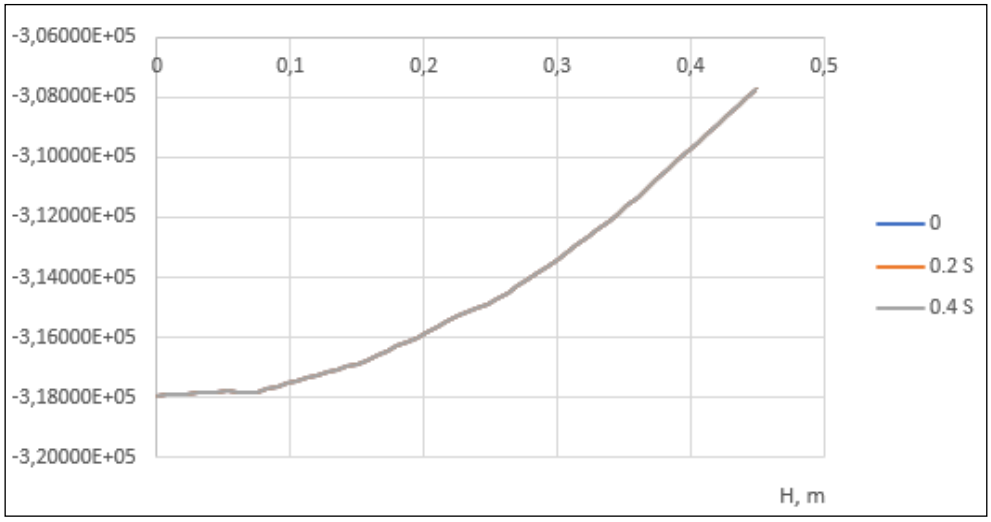

Figure 6

Vertical displacements with distance into the structure at parameter $a = 0, 0.2C, 0.4C$

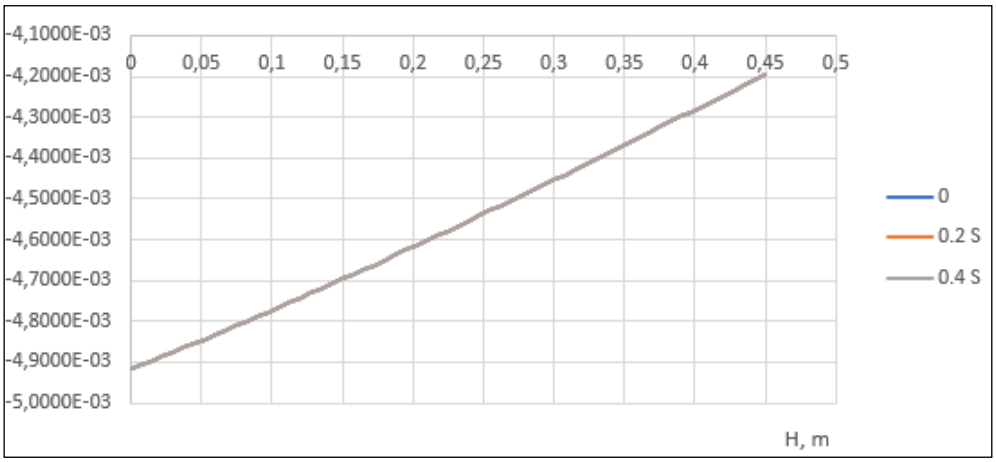

The character of distribution of elements of stress-strain state of the structure for two most different variants (Figures 7, 8): linear (b=0) and power potential (b=1.5).

In the case of a power potential, there is an increased value of vertical displacements and a slow decrease of this value in the upper part of the structure.

Figure 7

Vertical displacement diagram for linear potential (b=0), m

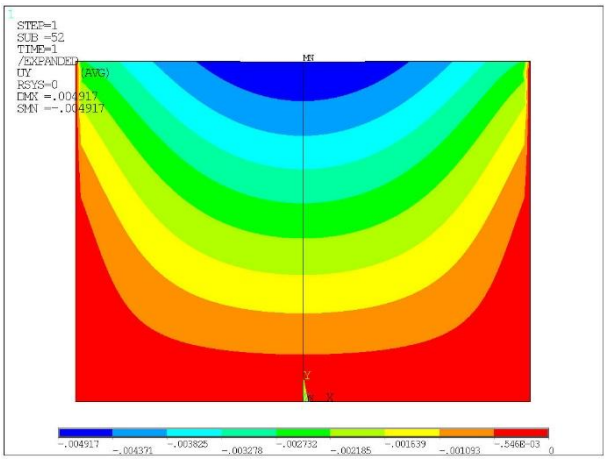

Figure 8

Vertical displacement diagram for a power potential (b=1.5), m

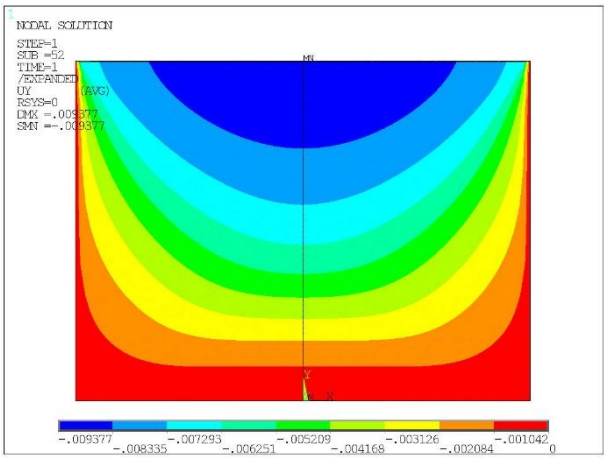

The diagrams of vertical compressive stresses (Figures 9, 10) show their more uniform distribution over the volume in the case of the step potential and less significant influence of boundary conditions at the vertical and lower boundaries of the region.

Figure 9

Diagram of vertical compressive stresses for linear potential (b=0), Pa

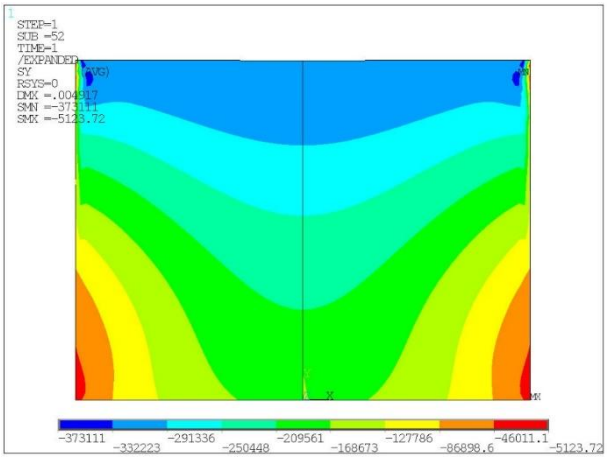

Figure 10

Diagram of vertical compressive stresses for the power potential (b=1.5), Pa

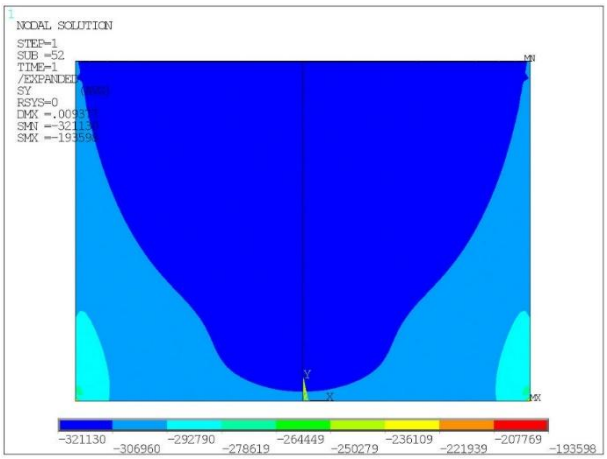

Significant differences are also observed in the distribution of stress intensity (Figures 11, 12).

Figure 11

Stress intensity diagram for linear potential (b=0), Pa

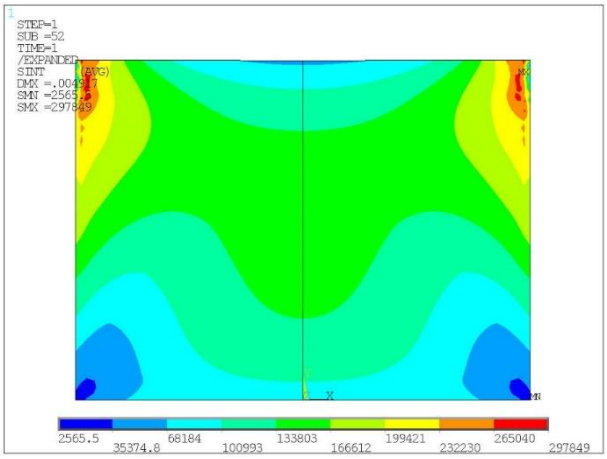

Figure 12

Stress intensity diagram for the power potential (b=1.5), Pa

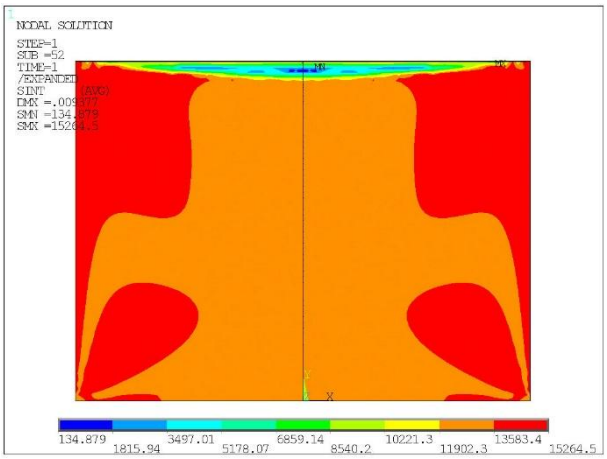

The linear potential is characterized by a significant concentration of stresses in the upper part of the structure near the vertical boundaries of the region, which should lead to a violation of the conditions of rigid bonding on them. For the power potential, the stress intensity is more uniform and the stress concentration is not pronounced. In this case, greater fluidity of the material is manifested. This is also confirmed by the distribution of hydrostatic pressure for the step potential (Figure 13).

Figure 13

Hydrostatic pressure diagram for power potential (b=1.5), Pa

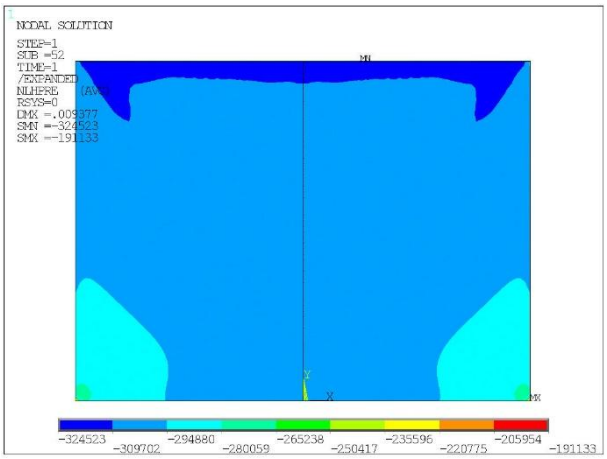

4 CONCLUSION

Thus, a numerical study of the nonlinear deformation of a sand mass at uniform surface pressure revealed a significant difference in the behavior of the material for the extended Drucker-Prager model with linear and power determination of the yield potential.

This difference can be used to describe the properties of a sandy base of a multilayer structure of a non-rigid type of pavement.

The refined model of the nonlinear behavior of soil and sandy substrate with the possibility of varying the properties and type of the model makes it possible to more accurately describe the processes of structural deformation and bring the model and experimental data into line.

5 RECOMMENDATIONS

It is recommended that the extended Drucker-Prager model with a power-law flow potential be considered for numerical simulations of non-rigid pavements on sandy subgrades. The choice of the flow potential type significantly influences the distribution of stresses and displacements; therefore, the model parameters should be calibrated against experimental data from specific site conditions to ensure accurate prediction of the stress-strain state.

SCIENTIFIC ETHICS DECLARATION

The authors declare that the scientific ethical and legal responsibility of this article published in EPSTEM journal belongs to the authors.

CONFLICT OF INTEREST

The authors declare that they have no conflicts of interest.

FUNDING

This research received no external funding.

ACKNOWLEDGEMENTS OR NOTES

This article was presented as an oral presentation at the International Conference on Basic Sciences and Technology (www.icbast.net) held in Konya/Türkiye on April 02-05, 2026.

REFERENCES

Abdullah, G.M.S. (2023) Performance of enhanced problematic soils in roads pavement structure: numerical simulation and laboratory study. *Sustainability*, *15*(3), 2595.

Alam, J.I., Lo, S.R., & Gnanendran, C.T. (2014) Numerical modeling of strain-softening response in triaxial testing of silty sand using FLAC2D. *Soil Behavior and Geomechanics, 236.* 606-614. https://doi.org/10.1061/9780784413388.063.

Altun, S., & Goktepe, A.B. (2006) Dependence of dynamic shear modulus of uniform sands on stress level and density. *Civil Engineering and Environmental Systems, 23*(2), 101-116.

Babushkina, N.E., & Lyapin, A.A. (2024) Determination of dynamic stresses and displacements under the action of an impact load on a two-layer structure during the indentation process. *Advanced Engineering Research (Rostov-on-Don). 24*(3). 264–273. https://doi.org/10.23947/2687-1653-2024-24-3-264-273

Bardet, J. P. (1990) Hypoplastic model for sands. *Journal of Engineering Mechanics, 116* (9), 1973-1994.

Fattah, M.Y., Hamood, M.J., & Abbas, S.A. (2013) Simulation of behavior of plate on elastic foundation under impact load by the finite element method. *Engineering and Technology Journal, 31*(19), 44-58.

Konorev, A.S., Mironchuk, S.A., Eremenko, E.A. & Podgornov, M.N. (2023) Road testing complex for accelerated testing of road pavements. *Dorogi i mosty , 2*(50). 43-60.

Kumar, J., & Madhusudhan, B.N. (2012) Dynamic properties of sand from dry to fully saturated states. *Geotechnique*, *62*(1), 45-54.

Liao, D., Hu, X., Wang, S., & Zhou, C. (2025) Improvement of a hypoplastic model for sand under undrained loading conditions. *Canadian Geotechnical Journal, 62*. https://doi.org/10.1139/cgj-2023-0670

Liu, K., Yin, Z.-Y., Chen, W.-B., Feng, W.-Q., & Yin, J.-H. (2021) Nonlinear model for the stress-strain-strength behavior of unsaturated granular materials. *International Journal of Geomechanics, 21*(7), 04021103.

Yin, Z.-Y., Wu, Z.-X., & Hicher, P.-Y. (2018) Modeling monotonic and cyclic behavior of granular materials by exponential constitutive function. *Journal of Engineering Mechanics, 144*(4). https://doi.org/10.1061/(ASCE)EM.1943-7889.0001437

Zhiqu, Lu, & Sabatier, J.M. (2008) Static and dynamic nonlinear behaviors of unconsolidated granular media. *Journal of the Acoustical Society of America, 123*, 3273.